

# Smooth surfaces from rational bilinear patches

Ling Shi <sup>1</sup>, Jun Wang <sup>1</sup> and Helmut Pottmann <sup>1,2</sup>

<sup>1</sup> King Abdullah University of Science and Technology, Thuwal 23955, Saudi Arabia

<sup>2</sup> Vienna University of Technology, 1040 Vienna, Austria

---

## Abstract

Smooth freeform skins from simple panels constitute a challenging topic arising in contemporary architecture. We contribute to this problem area by showing how to approximate a negatively curved surface by smoothly joined rational bilinear patches. The approximation problem is solved with help of a new computational approach to the hyperbolic nets of Huhnen-Venedey and Rörig and optimization algorithms based on it. We also discuss its limits which lie in the topology of the input surface. Finally, freeform deformations based on Darboux transformations are used to generate smooth surfaces from smoothly joined Darboux cyclide patches; in this way we eliminate the restriction to surfaces with negative Gaussian curvature.

*Keywords:* Discrete differential geometry, architectural geometry, fabrication-aware design, asymptotic net, hyperbolic net, rational bilinear patch, Darboux cyclide, Darboux transformation

---

## 1. Introduction

The growing interest of contemporary architects in freeform structures poses new challenges to digital design. In this area, there are numerous open problems, one of them being the production of smooth architectural freeform skins (surfaces). To make them affordable, they have to be composed of simple and easily manufacturable panels (patches). The manufacturing cost of a panel depends on the material and the process to produce it, which includes the production of the mold.

Let us look at an example: To produce a curved glass-fibre reinforced concrete panel, a mold is produced from styrofoam. The cheapest way of mold production is to use heated wire cutting, which can only produce ruled surfaces. Hence ruled panels are an advantage. Ruled surfaces are also advantageous

---

*Email address:* ling.shi(jun.wang,helmut.pottmann)@kaust.edu.sa (Ling Shi <sup>1</sup>, Jun Wang <sup>1</sup> and Helmut Pottmann <sup>1,2</sup>)

for the manufacturing of form work on which the concrete is poured, for sub-structures and for timber constructions.

Hence, as a contribution towards *fabrication-aware design*, we ask ourselves how to compose smooth surfaces from simple ruled patches. The simplest case, smooth surfaces from bilinear patches, has been investigated recently by Käferböck and Pottmann [1]. The resulting surfaces possess rather strong shape restrictions as they represent discrete versions of affine minimal surfaces previously introduced by Craizer et al. [2].

Can we do more with *rational* bilinear patches? It is clear that smoothly joined negatively curved patches will only generate models of negatively curved surfaces  $S$ . It turns out that the only remaining restriction is on the topology of  $S$ : the surface  $S$  has to be simply connected. As in many other instances of geometric problems in freeform architecture [3], we are again led to discrete differential geometry: Useful discrete representations of negatively curved surfaces are discrete asymptotic parameterizations, namely quad meshes with planar vertex stars (*A-nets*; see e.g. [4]). Huhnen-Venedey and Rörig [5] could show that simply connected *A-nets* (whose extraordinary vertices are of even valence) can be extended to smooth surfaces via rational bilinear patches (under a certain mild condition on the way how the quad strips in the mesh are twisted, which for a sufficiently fine *A-net* is satisfied anyway). They call the resulting structures *hyperbolic nets* (*H-nets*), as they are typically composed of hyperboloid patches (but may contain patches of hyperbolic paraboloids as well).

In the present paper, we further elaborate on hyperbolic nets by providing a new elementary derivation: While Huhnen-Venedey and Rörig [5] work in the Plücker quadric model of line geometry, we just use the rational Bézier form and thus also contribute to a simple computation based on standard CAGD methods. Moreover, we add a proper algorithmic treatment of surface approximation with *H-nets*, formulated within a global geometric optimization framework.

### 1.1. Previous work

Paneling freeform skins is an important issue in architecture. Eigensatz et al. [6] presented an optimization framework which allows one to achieve a good balance between production cost and skin quality, the latter being evaluated through the size of gaps and the kink angles occurring at adjacent panels. Ideally, these measures should be zero, but this is in general not achievable, unless the geometry and the panel seam layout are special.

Negatively curved smooth surfaces which are composed of ruled surface strips, have been addressed by S. Flöry et al. [7, 8, 9]. This work does not employ rational bilinear patches. It can be seen as a computational approach to semidiscrete asymptotic parameterizations, which have been investigated from a mathematical viewpoint by J. Wallner [10].

As we deal here with a smooth extension of a mesh, we point to the related problem of extending the vertices of a circular mesh (quad mesh all whose

quads possess a circum-circle) smoothly with Dupin cyclide patches [11]; a computational treatment of these cyclidic nets along with generalizations aiming at substructures in freeform architecture, has been presented by Bo et al. [12]. The theoretical beauty of the approach by Huhnen-Venedey and Rörig [5] lies in the use of the Plücker quadric model, which reveals the close relation to cyclidic nets, in accordance with the famous line-sphere transformation of S. Lie (which is of theoretical interest, but not directly applicable as it is not real). Independently from our work, Huhnen-Venedey and Schief [13] developed an affine approach to H-nets which is related to ours and which they use for the study of Weingarten transformations.

While cyclidic nets are always arranged along curvature lines, we may ask for generalizations by replacing Dupin cyclides by Darboux cyclides [14]. Like Dupin cyclides, the latter also contain families of circles (up to six!), which is an advantage for production on the large architectural scale. As a first step towards the most general Darboux cyclide patchworks we address here a simple computation from hyperbolic nets via so-called Darboux transformations.

## 1.2. Contributions and overview

The contributions of the present paper are as follows:

1. We provide a simple CAGD proof of the main result of Huhnen-Venedey and Rörig [5] along with formulae for computations based on the rational Bézier form (Section 2).
2. We show how to approximate a given negatively curved surface with a smooth union of rational bilinear patches, through a numerical optimization algorithm which combines A-net generation and its smooth extension with ruled quadric patches (Section 3).
3. We apply Darboux transformations to obtain smooth surfaces from Darboux cyclide patches; these surfaces are no longer restricted to negative Gaussian curvature (Section 4).

## 2. An elementary approach to hyperbolic nets

### 2.1. Some basics on rational bilinear patches

A rational bilinear patch with control points  $\mathbf{b}_0, \dots, \mathbf{b}_3$  and positive weights  $w_0, \dots, w_3$  is given by the parametric representation

$$\mathbf{x}(u, v) = \frac{(1-u)(1-v)w_0\mathbf{b}_0 + u(1-v)w_1\mathbf{b}_1 + (1-u)v w_3\mathbf{b}_3 + uv w_2\mathbf{b}_2}{(1-u)(1-v)w_0 + u(1-v)w_1 + (1-u)v w_3 + uv w_2}, \quad (1)$$

with  $(u, v) \in [0, 1]^2$ . One can obtain it from a bilinear patch  $\bar{\mathbf{x}}(u, v)$  in  $\mathbb{R}^4$ , with vertices  $\bar{\mathbf{b}}_i := (w_i\mathbf{b}_i, w_i)$ , by mapping it into 3-space with help of the canonical projection  $(x_1, \dots, x_4) \mapsto (x_1/x_4, x_2/x_4, x_3/x_4)$ . The patch lies on a ruled quadric and carries two families of straight line segments (rulings), namely the  $u$ - and  $v$ -isoparameter lines.

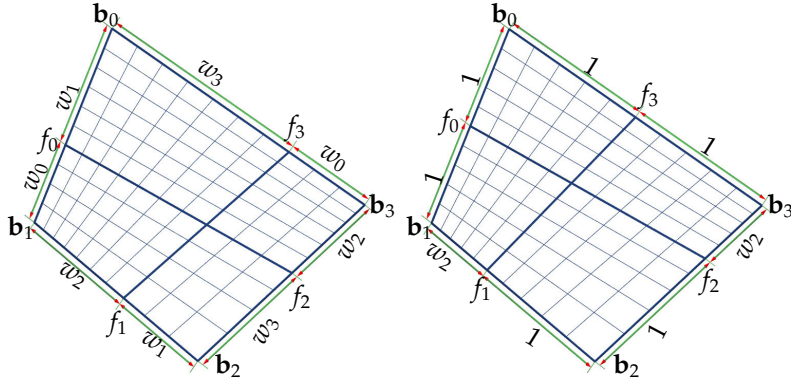


Figure 1: A rational bilinear patch lies on a ruled quadric. The frame points  $\mathbf{f}_i$  divide the edges in the inverse ratio of the corresponding vertex weights (left). Without loss of generality, one can set 3 of the four weights equal to 1 (right).

Let us first discuss why it is *sufficient to set three of the four weights equal to 1*, say

$$w_0 = w_1 = w_3 = 1, \quad (2)$$

without losing the possible variety of quadric patches with a given boundary polygon  $\mathbf{b}_0 \dots \mathbf{b}_3$ . One way of proving this uses the so-called *frame points* which are the canonical projections of the edge midpoints of  $\bar{\mathbf{x}}$ . These points  $\mathbf{f}_0 = \mathbf{x}(1/2, 0)$ ,  $\mathbf{f}_1 = \mathbf{x}(1, 1/2)$ ,  $\mathbf{f}_2 = \mathbf{x}(1/2, 1)$ ,  $\mathbf{f}_3 = \mathbf{x}(0, 1/2)$ , are expressed as  $\mathbf{f}_i := (w_i \mathbf{b}_i + w_{i+1} \mathbf{b}_{i+1}) / (w_i + w_{i+1})$  (with indices taken modulo 4). They divide the boundary edges in the inverse ratio of the corresponding weights (see Fig. 1, left). Frame points on opposite edges are connected by straight line segments which lie entirely on the patch  $\mathbf{x}$  (isoparameter lines  $u = 1/2$  and  $v = 1/2$ , respectively). A given ruled quadric patch has infinitely many rational bilinear parameterizations: We can choose a ruling in each of the two families as those connecting the frame points, and this determines the weights and hence the parameterization of the patch. Let us choose rulings so that two frame points on adjacent edges, say  $\mathbf{f}_0, \mathbf{f}_3$ , are edge midpoints (Fig. 1, right). This implies  $w_0 = w_1 = w_3$ , and as only the ratio of weights matters, we can set these three weights to 1. Hence we are left with a single “shape parameter”, the weight  $w_2$ , in accordance with the fact that there is only a one-parameter family of ruled quadric patches through a given skew quadrilateral with vertices  $\mathbf{b}_0, \dots, \mathbf{b}_3$ . Note that  $w_2 = 1$  characterizes a patch of a hyperbolic paraboloid; otherwise the patch lies on a one-sheeted hyperboloid.

While it is convenient for some of our discussions to have three weights equal to 1, we also need to convert to the general case: *Two rational bilinear patches with the same control points and weights  $w_i$  and  $w'_i$ , respectively, define the*

same quadric patch, if and only if

$$\frac{w_0 w_2}{w_1 w_3} = \frac{w'_0 w'_2}{w'_1 w'_3}. \quad (3)$$

This follows easily from projective geometry, namely the fact that the cross ratios determined by control points and frame points on one pair of opposite edges of the control quad have to agree (then they also agree on the other edge pair),

$$\text{cr}(\mathbf{b}_1, \mathbf{b}_2, \mathbf{f}_1, \mathbf{f}'_1) = \text{cr}(\mathbf{b}_0, \mathbf{b}_3, \mathbf{f}_3, \mathbf{f}'_3),$$

which is equivalent to (3) and once again shows that we can set three of the weights equal to 1. If the value

$$W := \frac{w_0 w_2}{w_1 w_3} \quad (4)$$

approaches 0 or  $\infty$ , the patch exhibits increasing curvature along a diagonal of the control quad, and in the limit it becomes a pair of triangles. As this is very undesirable for our applications, we want  $W$  to be sufficiently close to 1, which we will later use in our optimization algorithm. Note that the value  $W$  depends on the selection of a diagonal in the quad. The product of weights of the vertices of this diagonal are in the numerator. Depending on the diagonal selection, the value of the shape parameter is  $W$  or  $1/W$ .

## 2.2. Smoothly joining two rational bilinear patches along a common edge

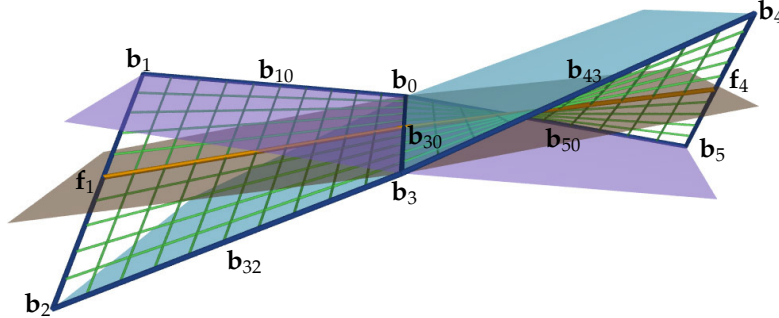


Figure 2: Two rational bilinear patches, joined smoothly along a common edge, together with auxiliary planes used in Proposition 1 and its proof.

Using the notation from Fig. 2, we prove a simple condition for smoothly joined rational bilinear patches:

**Proposition 1.** *Let us consider two rational bilinear patches with vertices  $\mathbf{b}_0, \mathbf{b}_1, \mathbf{b}_2, \mathbf{b}_3$  and  $\mathbf{b}_0, \mathbf{b}_3, \mathbf{b}_4, \mathbf{b}_5$ , and weights  $w_i$  of  $\mathbf{b}_i$  equal to one, except weights  $w_2$  and  $w_4$ . Then these patches join smoothly along the common edge  $\mathbf{b}_0\mathbf{b}_3$  if the vertex stars at the*

common vertices are planar, i.e., points  $\mathbf{b}_0, \mathbf{b}_1, \mathbf{b}_3, \mathbf{b}_5$  and  $\mathbf{b}_0, \mathbf{b}_2, \mathbf{b}_3, \mathbf{b}_4$  are coplanar, and if the following condition holds,

$$w_2 \det(\mathbf{b}_{30}, \mathbf{b}_{50}, \mathbf{b}_{20}) = w_4 \det(\mathbf{b}_{30}, \mathbf{b}_{10}, \mathbf{b}_{40}), \quad \text{with } \mathbf{b}_{ij} := \mathbf{b}_i - \mathbf{b}_j. \quad (5)$$

*Proof.* It is well known that two ruled surfaces join smoothly along a common ruling as soon as we have agreement of tangent planes at three points of that ruling. Two of these points are  $\mathbf{b}_0, \mathbf{b}_3$ , and so we just need to ensure a common tangent plane at a third point. We choose the frame point  $(\mathbf{b}_0 + \mathbf{b}_3)/2$  and get the condition

$$\det\left(\mathbf{b}_{30}, \frac{\mathbf{b}_1 + w_2 \mathbf{b}_2}{1 + w_2} - \frac{\mathbf{b}_0 + \mathbf{b}_3}{2}, \frac{\mathbf{b}_5 + w_4 \mathbf{b}_4}{1 + w_4} - \frac{\mathbf{b}_0 + \mathbf{b}_3}{2}\right) = 0.$$

This equation can be rewritten as

$$\det(\mathbf{b}_{30}, \mathbf{b}_{10} + \mathbf{b}_{13} + w_2 \mathbf{b}_{23} + w_2 \mathbf{b}_{20}, \mathbf{b}_{50} + \mathbf{b}_{53} + w_4 \mathbf{b}_{43} + w_4 \mathbf{b}_{40}) = 0,$$

and by adding  $(1 + w_2)\mathbf{b}_{30}$  to the 2nd vector and  $(1 + w_4)\mathbf{b}_{30}$  to the third, we arrive at

$$\det(\mathbf{b}_{30}, 2\mathbf{b}_{10} + 2w_2 \mathbf{b}_{20}, 2\mathbf{b}_{50} + 2w_4 \mathbf{b}_{40}) = 0.$$

Due to the planarity constraints at  $\mathbf{b}_0$  and  $\mathbf{b}_3$ , we have  $\det(\mathbf{b}_{30}, \mathbf{b}_{10}, \mathbf{b}_{50}) = \det(\mathbf{b}_{30}, \mathbf{b}_{20}, \mathbf{b}_{40}) = 0$  and this reduces the condition to equation (5).  $\diamond$

**Remark 2.** Positive weights  $w_2, w_4$  for the smoothly joined patches require equal sign of the two determinants  $\det(\mathbf{b}_{30}, \mathbf{b}_{50}, \mathbf{b}_{20})$  and  $\det(\mathbf{b}_{30}, \mathbf{b}_{10}, \mathbf{b}_{40})$  (called *equitwist condition* in [5]). Let us denote the tangent planes of the vertex stars at  $\mathbf{b}_0$  and  $\mathbf{b}_3$  by  $T_0$  and  $T_3$ , respectively. Then, a practically useful net will have (i)  $\mathbf{b}_1$  and  $\mathbf{b}_5$  on different sides of the common edge  $\mathbf{b}_0\mathbf{b}_3$  (inside plane  $T_0$ ) and (ii)  $\mathbf{b}_2$  and  $\mathbf{b}_4$  on different sides of  $\mathbf{b}_0\mathbf{b}_3$  (inside plane  $T_3$ ); the latter implies that  $\mathbf{b}_2$  and  $\mathbf{b}_4$  are on different sides of  $T_0$ , and thus the sign condition is satisfied. Hence, ensuring positive weights does not cause any problems in the practical computations discussed below.

**Remark 3.** For general weights  $w_i$ , we obtain in view of (3) the following condition for a smooth connection,

$$w_2 w_5 \det(\mathbf{b}_{30}, \mathbf{b}_{50}, \mathbf{b}_{20}) = w_1 w_4 \det(\mathbf{b}_{30}, \mathbf{b}_{10}, \mathbf{b}_{40}). \quad (6)$$

We can nicely rewrite this condition in terms of the shape parameters  $W$  defined in (4). Selecting the diagonal  $\mathbf{b}_0\mathbf{b}_2$  for the left patch, we define the shape parameter  $W_l := w_0 w_2 / w_1 w_3$ . Selecting the diagonal  $\mathbf{b}_0\mathbf{b}_4$  for the right patch, we have  $W_r := w_0 w_4 / w_3 w_5$ . Then, (6) can be rewritten as

$$\frac{W_r}{W_l} = \frac{\det(\mathbf{b}_{30}, \mathbf{b}_{50}, \mathbf{b}_{20})}{\det(\mathbf{b}_{30}, \mathbf{b}_{10}, \mathbf{b}_{40})}. \quad (7)$$

Hence, any two smoothly joined pairs of quadric patches have shape parameters with a constant ratio,  $W_r : W_l = W'_r : W'_l$ , which is determined by the control points alone.

### 2.3. Smooth extension of an A-net

We allow *extraordinary vertices*  $\mathbf{v}$  (with planar vertex star) in an A-net, but note that they must be of *even valence*. This is so, since the quads assembled around a vertex  $\mathbf{v}$  have their free vertex (the one which is not connected to  $\mathbf{v}$  by an edge) alternately on different sides of the tangent plane  $T$  at  $\mathbf{v}$  (see Remark 2).

We are now in a position to provide a simple proof of the main result of Huhnen-Venedey and Rörig [5].

**Theorem 4.** *Any simply connected A-net whose interior vertices are of even valence and which satisfies the equitwist condition (cf. Remark 2) possesses a one-parameter family of smooth extensions to a hyperbolic net (patchwork of smoothly joined rational bilinear patches).*

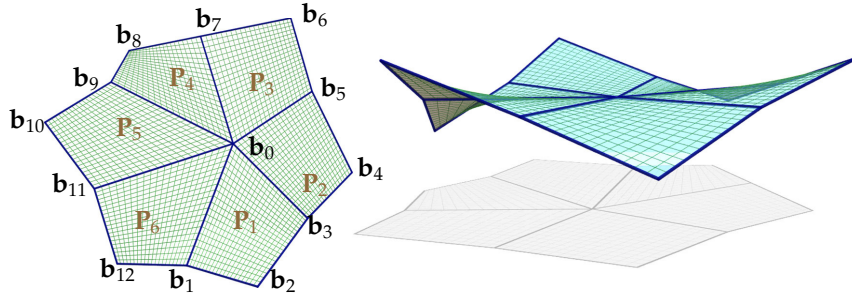


Figure 3: Smoothly joined rational bilinear patches, assembled around a common vertex.

*Proof.* We arbitrarily fill a patch into one quad of the A-net and then obtain the others through application of the smoothness condition (5). As we have a simply connected A-net, there are no global closure problems. Hence, it is sufficient to prove consistency around vertices. At a vertex  $\mathbf{b}_0$  of even valence  $n$ , we have to ensure that successive patches  $P_i$  and  $P_{i+1}$  meet smoothly,

$$w_{2i} \det(\mathbf{b}_{2i+1,0}, \mathbf{b}_{2i+3,0}, \mathbf{b}_{2i,0}) = w_{2i+2} \det(\mathbf{b}_{2i+1,0}, \mathbf{b}_{2i-1,0}, \mathbf{b}_{2i+2,0}), \quad i = 1, \dots, n, \quad (8)$$

where indices are taken modulo  $2n$  (see Fig. 3). Starting to fill in patch  $P_1$ , i.e., selecting  $w_2$ , these smoothness conditions yield  $w_4, w_6, \dots, w_{2n}$ , and then the last patch  $P_n$  must join smoothly with  $P_1$  along  $\mathbf{b}_0\mathbf{b}_1$ . This amounts to the closure condition

$$\prod_{i=1}^n \det(\mathbf{b}_{2i+1,0}, \mathbf{b}_{2i+3,0}, \mathbf{b}_{2i,0}) = \prod_{i=1}^n \det(\mathbf{b}_{2i+1,0}, \mathbf{b}_{2i-1,0}, \mathbf{b}_{2i+2,0}). \quad (9)$$

A determinant is a signed volume of a parallelepiped. Fixing an orientation of the tangent plane  $T_0$  at  $\mathbf{v}_0$ , we consider the signed area  $A_i$  of the parallelogram defined by  $\mathbf{b}_{2i-1,0}, \mathbf{b}_{2i+1,0}$  and the signed distance  $d_i$  of  $P_i$ 's free vertex  $\mathbf{b}_{2i}$  from  $T_0$ . Then, we have

$$\det(\mathbf{b}_{2i+1,0}, \mathbf{b}_{2i+3,0}, \mathbf{b}_{2i,0}) = A_{i+1}d_i, \quad \det(\mathbf{b}_{2i+1,0}, \mathbf{b}_{2i-1,0}, \mathbf{b}_{2i+2,0}) = -A_i d_{i+1},$$

so that left and right hand side of (9) are equal, since  $n$  is even.  $\diamond$

**Remark 5.** We have seen that there is a one-parameter family of smooth extensions of an A-net. The shape parameters  $W_i$  of these solutions are very closely related: To see this, let us select diagonals in the A-net so that diagonals of quads with a common edge meet at a common vertex of that edge. In view of equation (7), we just need to compute one set of parameters, say  $(W_0, W_1, \dots)$ . Any other solution must have the same ratio of shape parameters and thus be of the form  $\lambda \cdot (W_0, W_1, \dots)$ .

### 3. Approximating a negatively curved surface with smoothly joined rational bilinear patches

In this section, we show how to approximate a simply connected, negatively curved surface  $S$  (given as a triangle mesh) by a hyperbolic net  $\mathcal{H}$ . This includes a global optimization algorithm which we use to get high quality results for problems where we have direct constructions, like extending an A-net to an H-net. Moreover, optimization can be employed also in scenarios where we have no theoretical guarantee that an H-net exists; this is illustrated by surfaces  $S$  that are not of disk topology.

The computational pipeline of the approximation algorithm is as follows:

- Compute the frame field of asymptotic directions of the input surface  $S$  and approximate  $S$  by a quad mesh  $Q$  which follows the asymptotic directions (subsection 3.1).
- Optimize  $Q$  to a hyperbolic net  $\mathcal{H}$  approximating  $S$  (subsection 3.2).

#### 3.1. Approximating a negatively curved surface with a quad mesh guided by the frame field of asymptotic directions

*Initialization: computing the asymptotic directions.* Given a triangle mesh  $S$ , we firstly estimate the curvature tensor for the barycenter of each face by the 3rd order jet fit of Cazals and Pouget [15] and compute the asymptotic directions from it. These asymptotic directions can be considered as a special frame field. Singularities of the asymptotic direction field occur at flat points of the surface  $S$ , therefore they are also singularities of the principal direction field. Singularities of a frame field are classified via the cross field of bisectors (in our case, principal directions), and thus – as for the principal direction field – the indices of the asymptotic field are integer multiples of  $1/2$  (for a proof, see e.g. [16]). However, we can show even more (for a proof, see the Appendix):

**Theorem 6.** *An ordinary flat point (i.e., a surface point whose tangent plane has 2nd order contact with the surface, but not 3rd order contact) which lies inside a surface region with negative Gaussian curvature, is a singularity of index  $-1/2$  for the principal field and the asymptotic field.*

It has to be expected that higher order flat points can be seen as limit cases of several nearby ordinary flat points. Since indices in an area add up, we conjecture that the index is always negative. For rationalization of freeform structures, the non-generic case is very unlikely to appear: According to Smyth and Xavier [17], umbilics with an index different from  $\pm 1/2$  are critical points of Gaussian curvature  $K$ , mean curvature  $H$  and, additionally, the 3-jet of  $H^2 - K$  vanishes there.

*Quad re-meshing guided by the asymptotic direction field.* Once we have the asymptotic directions on each face, we re-mesh  $S$  to obtain a quad mesh  $\mathcal{Q}$  whose edges follow the asymptotic directions. We can make use of quad re-meshing algorithms such as *QuadCover* [18] or *mixed-integer quadrangulation* [19]. In our implementation, we adopt the method of Liu et al. [20], which is a version of mixed-integer quadrangulation.

Since we aim at the optimization of  $\mathcal{Q}$  towards an A-net that is extendable to an H-net, we have to make sure that all inner vertices of  $\mathcal{Q}$  have even valence. As discussed above, a flatpoint of the input surface  $S$  will most likely be an ordinary one (index  $-1/2$ ) and thus lead to a vertex of valence 6. If our conjecture that the index is always negative holds true, we would only get even valences and thus be able to model all cases.

### 3.2. Optimization of a quad mesh towards a hyperbolic net

In a quad mesh  $\mathcal{Q}$  which follows the asymptotic field, the vertex stars are nearly planar, and thus  $\mathcal{Q}$  serves as a good initialization for optimization towards an A-net  $\mathcal{A}$  and subsequently towards an H-net  $\mathcal{H}$ . We proceed as follows (see the flowchart in Figure 4):

1. Taking the quad mesh  $\mathcal{Q}$  as input, we optimize it towards an A-net  $\mathcal{A}$ , i.e., we flatten its vertex stars while keeping fairness and proximity to the reference surface  $S$ .
2. We extend the A-net  $\mathcal{A}$  to a hyperbolic net  $\mathcal{H}$  by computing the best possible shape parameters, avoiding unnecessarily high mean curvature in patches. This step has an explicit solution.
3. We fix the shape parameters and update mesh vertices by a global optimization of the H-net  $\mathcal{H}$  to achieve an even better curvature behavior and satisfaction of constraints to higher precision. This step is iterated with the 2nd step, as illustrated in Figure 4.

These steps are detailed below.

*Step 1: Optimization towards an A-net.* The quad mesh  $\mathcal{Q}$  provides a good initialization for optimization towards an A-net  $\mathcal{A}$ , which we obtain by minimizing the following objective function,

$$\mathbf{F}_{anet}(\mathbf{b}) = \sum_i F_p(\mathbf{b}_i) + \lambda_1 F_{fairness} + \lambda_2 F_{prox}. \quad (10)$$

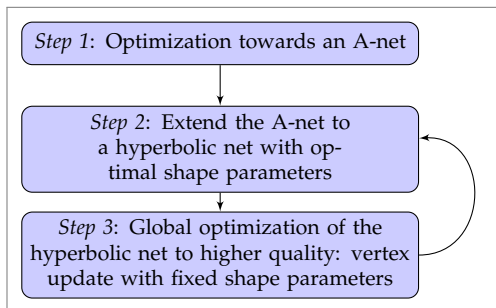


Figure 4: Overview of the optimization of a quad mesh (which follows the asymptotic field of a reference surface) towards a hyperbolic net. We iterate step 2 and step 3 several times to achieve better curvature behavior and to satisfy constraints to higher accuracy. This is particularly important when we apply the algorithm to surfaces which are not simply connected.

Here  $F_p(\mathbf{b}_i)$  ensures planarity of the vertex star around vertex  $\mathbf{b}_i$ ,  $F_{fairness}$  aims at high mesh fairness and  $F_{prox}$  makes sure that the mesh stays close to the reference surface  $S$ .

The *proximity* term  $F_{prox}$  is composed of two parts: the squared distance of each vertex  $\mathbf{b}_i$  to its closest point  $\mathbf{b}_i^c$  on  $S$  and the squared distance of  $\mathbf{b}_i$  to the tangent plane of  $S$  at  $\mathbf{b}_i^c$ . This yields a good approximation of the squared distance function of  $S$ , especially in our case, where one is close to  $S$  and gives the tangent plane distance a higher weight (see e.g. [21]).

*Fairness* is achieved with an energy  $F_{fairness}$  which is a sum of squares of second or third order differences at vertices of all those mesh polylines which should be fair; we follow Deng et al. [22].

To handle *planarity of vertex stars*, we have two options: (i) We can add to each mesh vertex  $\mathbf{b}_i$  a vertex normal  $\mathbf{n}_i$  as additional variable and in this way define the plane of the vertex star. Then  $F_p$  is the sum of squared plane distances of direct neighbor vertices (see [22]). (ii) Planarity of a vertex star is expressed by planarity of a number of quads, where quad planarity is measured by the squared diagonal distance  $d^2$ . In fact, as a planarity measure of a quad  $\mathbf{b}_0, \dots, \mathbf{b}_3$  we only employ the following approximation of  $d^2$ ,

$$F_{quad}(\mathbf{b}_0, \mathbf{b}_1, \mathbf{b}_2, \mathbf{b}_3) = (\mathbf{n} \cdot \mathbf{d})^2,$$

where  $\mathbf{n} = (\mathbf{b}_{02} \times \mathbf{b}_{13}) / \|\mathbf{b}_{02} \times \mathbf{b}_{13}\|$  is a unit vector orthogonal to both diagonals and  $\mathbf{d} := (\mathbf{b}_0 + \mathbf{b}_2 - \mathbf{b}_1 - \mathbf{b}_3)/2$ . Obviously, to achieve planarity of a vertex star of valence  $n$ , we need to ensure planarity of  $n - 2$  quads. This is the approach taken in our implementation.

For numerical optimization, we use a Gauss-Newton method. At the end of this step, we have an A-net  $\mathcal{A}$ .

*Step 2: Extend the A-net to a hyperbolic net with optimal shape parameters.* Based on the smoothness condition (7) and Remark 5, we can easily extend an A-net  $\mathcal{A}$  to an H-net  $\mathcal{H}$  by computing the shape parameter  $W_i$  of each patch  $P_i$ . Starting at an arbitrary patch  $P_0$  to which we assign an initial parameter  $W_0^0 = 1$ , we move to neighboring faces and compute via (7) their shape parameters. This results in an initial set of parameters  $(W_0^0, W_1^0, \dots)$ . Any other shape parameter set is of the form  $\lambda \cdot (W_0^0, W_1^0, \dots)$ . To determine the optimal factor  $\lambda$ , we try to achieve patches whose shape parameter  $W_i$  is not close to 0 or  $\infty$ . This is achieved by minimizing

$$\mathbf{F}_{shape} = \sum_i [(W_i - 1)^2 + (\frac{1}{W_i} - 1)^2],$$

or equivalently

$$\mathbf{F}_{shape}(\lambda) = \sum_i [(\lambda W_i^0 - 1)^2 + (\frac{1}{\lambda W_i^0} - 1)^2]. \quad (11)$$

Minimization of this univariate function amounts to computing the roots of a quartic polynomial and thus this problem has an explicit solution.

*Step 3: Global optimization of the hyperbolic net  $\mathcal{H}$  to higher quality.* This step is taken for two reasons. (i) Numerical optimization is limited to a certain accuracy and thus vertex stars in  $\mathcal{A}$  are not fully planar, resulting in small deviations from smooth patch joints in  $\mathcal{H}$ . (ii) More importantly, the shape parameters for  $\mathcal{H}$  are computed from a given  $\mathcal{A}$ , and there is hope that by slightly changing  $\mathcal{A}$  we get an even better curvature behavior of the quadric patches in  $\mathcal{H}$ .

The entire global optimization of  $\mathcal{H}$  alternates between Step 3, which updates the mesh vertices (shape parameters fixed) and Step 2 (which updates shape parameters, but keeps vertices fixed). Here, we only have to discuss the update of vertices in  $\mathcal{H}$ . We want to jointly address the A-net property and smoothness of patch joints (with fixed weights). For a smooth joint of two patches along an edge, say  $\mathbf{b}_0, \mathbf{b}_3$ , frame points  $\mathbf{f}_1, \mathbf{f}_4$  should be co-planar with that edge, see Fig 2. Hence, we add an extra planarity term for the frame points. Recall that the frame points are computed from the weights (shape parameters), which are fixed in this step. Summarizing, the target functional is

$$\mathbf{F}_{frame}(\mathbf{b}) = \mathbf{F}_{anet}(\mathbf{b}) + \lambda_3 \sum_j F_{quad}(\mathbf{b}_0^j, \mathbf{f}_1^j, \mathbf{b}_3^j, \mathbf{f}_4^j).$$

Here the superscript  $j$  is used to enumerate all adjacent quad faces (inner edges).

### 3.3. Results and discussion

We provide a number of examples which partially go beyond the limits of the theory and demonstrate the capabilities and limitations of our optimization framework.

*Evaluation of smoothness.* For visualization of surface quality, we provide a sensitive analysis tool, namely *isophotes*. Isophotes are those curves on a surface  $\Phi$  along which the angle between the surface normal and a given fixed vector is constant. Thus, isophotes are typically one differentiation class below that of the surface. In particular, for a smooth (tangent plane continuous) surface  $\Phi$ , isophotes are continuous, but in general exhibit tangent discontinuities at curvature discontinuities of  $\Phi$ . Discontinuities in isophotes belong to tangent plane discontinuities of  $\Phi$ .

*Example 1: Simply connected surfaces.* Results of our optimization on simply connected surfaces are depicted in Figure 5. We can clearly see the smoothness of the surfaces. In fact, isophotes do not exhibit large kinks, indicating that the surfaces are in most parts nearly curvature continuous. This is also confirmed by the mean curvature plots in Figure 6, which further show that only few patches are highly curved at a diagonal.

*Example 2: Going beyond simply connected surfaces.* To test the limits of optimization, we applied the algorithm to surfaces which are not simply connected. As Figure 7 shows, the resulting H-nets of non-simply connected surfaces can be reasonably smooth. The kink angles are shown in Table 1. These mild deviations from smoothness are visible in partially rather strong discontinuities of isophotes. Figure 7 shows three minimal surfaces which are not simply connected.

*Example 3: Approximating a real data set.* We use a part of a design by Zaha Hadid Architects for the Cagliari Contemporary Arts Center project. The model is basically a negatively-curved surface. However, small parts of the model are nearly flat or of positive Gaussian curvature. We model it with a fixed boundary curve, but allow a higher deviation from the reference surface in the areas of non-negative Gaussian curvature. The resulting H-net is shown by Figure 8.

We also show the optimization details of our examples in Table 1. As expected, the simply connected surfaces require a smaller number of patches to achieve a good approximation, while the surfaces with multiple connections need larger H-nets and still produce higher kink angles.

Table 1: Optimization details for our examples. Here,  $|F|$  and  $|V|$  denote the number of faces and vertices, respectively;  $\lambda_1, \lambda_2, \lambda_3$  are the weights in the objective functions used for optimization, see 3.2;  $\alpha_{max}$  and  $\alpha_{mean}$  are the maximum and mean value of kink angles at patch joints.

Examples	$ F $	$ V $	$\lambda_1$	$\lambda_2$	$\lambda_3$	$\alpha_{max}$	$\alpha_{mean}$
mass spring surface	247	214	0.6	0.10	0.6	0.417	0.046
minimal surface 1	139	168	0.86	0.08	0.60	0.439	0.063
minimal surface 2	84	105	0.86	0.12	0.65	0.044	0.009
minimal surface 3	754	840	0.56	0.03	0.60	6.101	0.400
catenoid	1320	1408	0.40	0.02	0.60	3.316	0.850
Schwarz surface	702	802	0.60	0.04	0.60	4.553	0.542
Cagliari model	1623	1741	0.76	0.02	0.80	4.322	0.534

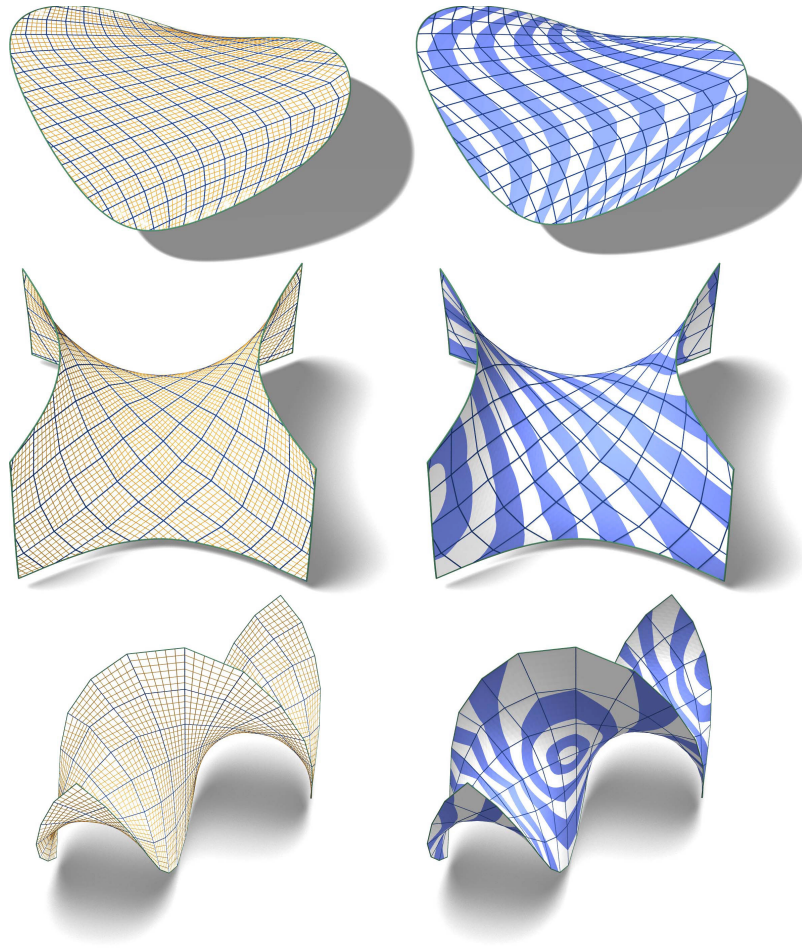


Figure 5: H-nets approximating simply connected surfaces. Left: H-nets, showing patches with some rulings. Right: Isophotes are continuous, confirming smoothness of the surface composed of rational bilinear patches. From top to bottom: “mass spring” surface, minimal surface 1 and minimal surface 2.

#### 4. Smoothly joined Darboux cyclide patches via Darboux transformation

Using smoothly joined ruled patches we can only model negatively curved surfaces. In order to get rid of this restriction, we need more general patches. Next to straight lines, circular arcs are probably easiest to manufacture, and thus we look for patches which carry two families of circular arcs. Darboux cyclide patches are good candidates for this task, especially since they can easily be obtained from ruled quadric patches (see e.g. [14], in particular Proposition 9). For our purposes it is sufficient to realize that so-called *Darboux transformations* (discussed below) transform ruled quadrics into Darboux cyclides (Remark 10

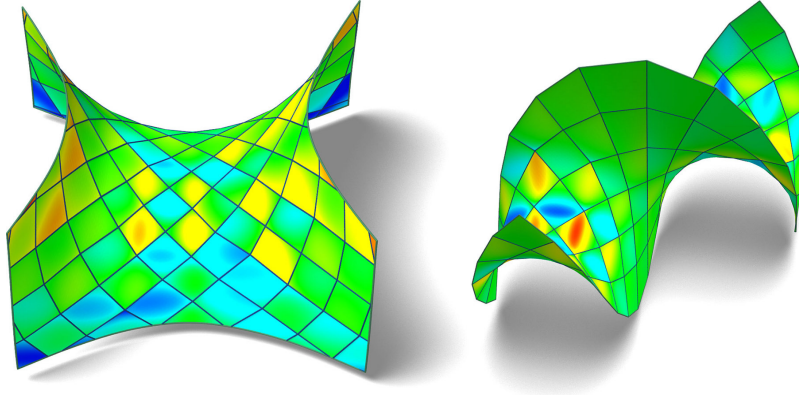


Figure 6: Mean curvature analysis of H-nets computed to minimal surfaces 1 and 2 from Figure 5. Here green color shows that the mean curvature  $H$  is close to zero. Red color indicates positive  $H$ , blue color belongs to negative  $H$ .

in [14]). Therefore, they transform hyperbolic nets to smooth surfaces composed of Darboux cyclide patches.

Darboux transformations occur in non-Euclidean geometry, where they are used for the transfer from the projective model of elliptic or hyperbolic geometry to the corresponding conformal model. Without reference to non-Euclidean geometry we may define them in 3D as follows: Embed points  $\mathbf{x} \in \mathbb{R}^3$  into 4-space  $\mathbb{R}^4$ , e.g. as  $(\mathbf{x}, 1)$ , and project them from a center  $C$  onto the unit sphere  $\Sigma : x_1^2 + \dots + x_4^2 = 1$ . Then, perform stereographic projection  $\sigma$  of  $\Sigma$ . We choose the projection center  $C$  as  $(0, 0, 0, c)$  with  $c \neq 1$ . Then, the straight line connecting  $C$  and  $(\mathbf{x}, 1)$  is parameterized as  $(\lambda \mathbf{x}, c + \lambda(1 - c))$ . Its intersection points with  $\Sigma$  are characterized by

$$\lambda = \frac{c^2 - c \pm \sqrt{(c-1)^2 + (1-c^2)\mathbf{x}^2}}{\mathbf{x}^2 + (c-1)^2}.$$

Stereographic projection from center  $(0, 0, 0, 1)$  onto  $x_4 = 0$  is given by

$$\sigma : (x_1, \dots, x_4) \mapsto (x_1, x_2, x_3)/(1 - x_4),$$

and thus we obtain for the Darboux transformation,

$$\mathbf{x} \mapsto \frac{\lambda \mathbf{x}}{(1-c)(1-\lambda)}.$$

We prefer to scale the image with  $1 - c$ , and this finally yields the Darboux transformation

$$\delta : \mathbf{x} \mapsto \frac{c^2 - c \pm \sqrt{(c-1)^2 + (1-c^2)\mathbf{x}^2}}{\mathbf{x}^2 + 1 - c \mp \sqrt{(c-1)^2 + (1-c^2)\mathbf{x}^2}} \cdot \mathbf{x}. \quad (12)$$

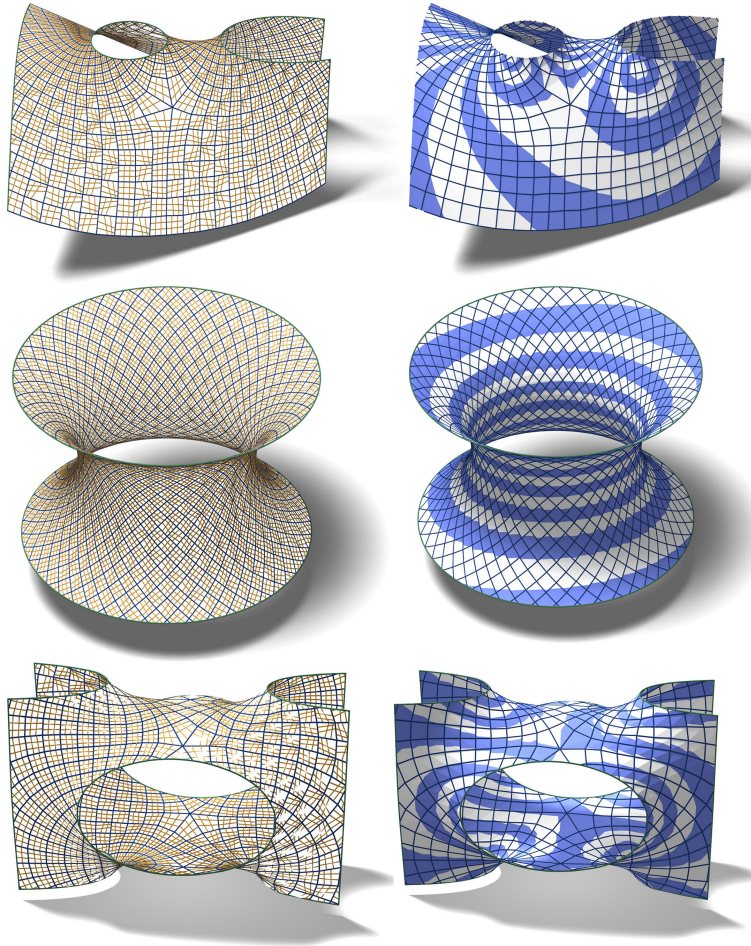


Figure 7: H-nets approximating multiply connected pieces of minimal surfaces. Left: H-nets with rulings. Right: isophotes exhibit some discontinuities, which points to tangent plane discontinuities. From top to bottom: minimal surface 3, catenoid and Schwarz surface.

By construction, the two image points  $\delta(\mathbf{x})$  are related to each other by an inversion with respect to a (not necessarily real) sphere  $\Lambda$ . This sphere is obtained as follows: Intersect the polar hyperplane  $x_4 = 1/c$  of  $C$  with respect to  $\Sigma$  with  $\Sigma$ ; this results in general ( $C \notin \Sigma$ , i.e.  $c \neq -1$ ) in a real or imaginary sphere  $\subset \Sigma$  whose stereographic image has the equation  $x_1^2 + x_2^2 + x_3^2 = (c+1)/(c-1)$ . After scaling with  $1-c$ , we arrive at the sphere  $\Lambda : x_1^2 + x_2^2 + x_3^2 = c^2 - 1$ .

It is appropriate to use Möbius geometry in image space, i.e., consider straight lines as circles and planes as spheres. Then we can state: A Darboux transformation maps a straight line to a Möbius circle and a plane to a Möbius

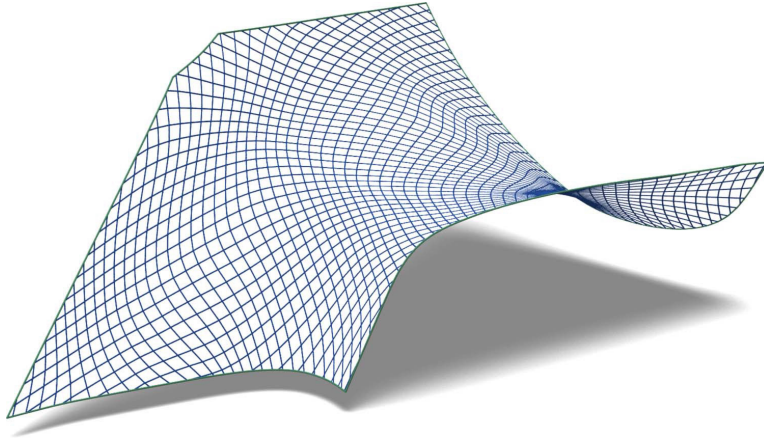


Figure 8: H-net approximation of part of the design surface of the Cagliari Art Center by Zaha Hadid Architects. We model the A-net with fixed boundary and allow part of the net to go beyond the reference surface (in areas where it is not negatively curved).

sphere (these circles and spheres are orthogonal to  $\Lambda$ ). If the center  $C$  is not inside  $\Sigma$  ( $|c| > 1$ ), these images need not be real. If  $C$  lies on  $\Sigma$  ( $c = -1$ ),  $\delta$  becomes an inversion. To get the most general Darboux transformations, we may at first apply a projective map in 3-space and then the mapping (12).

The most important property for our purposes is the fact that a rational bilinear patch is mapped to a pair of Darboux cyclide patches (inverse with respect to the sphere  $\Lambda$ ) and thus *a hyperbolic net is mapped to a pair of smooth surfaces composed of Darboux cyclide patches*.

We implemented a free-form deformation tool based on Darboux transformations. The H-net to be transformed is embedded in a box acting as a control cage. The cage is then deformed exploiting the 16 degrees of freedom (15 for the choice of an initial projective transformation and 1 for  $c$ ). Note that the transformed cage pair has circular edges and spherical faces. The transformation of the cage allows one to get a better feeling of the way how  $\delta$  will transform an object embedded in it. Examples are shown in Figure 9.

#### *Conclusion and future work*

Applying CAGD methods to a very recent development in discrete differential geometry, namely H-nets, and combining it with numerical optimization, we showed how to approximate a given negatively curved surface  $S$  with a smooth surface composed of ruled quadric patches. Limitations have been discussed and the applicability of the optimization framework beyond theoretical guarantees has been tested. Through Darboux transformations, we obtained a first method for smoothly joining Darboux cyclide patches.

Smooth or approximately smooth patchworks from Darboux cyclides will require further studies; in particular, we did not yet show how to approximate

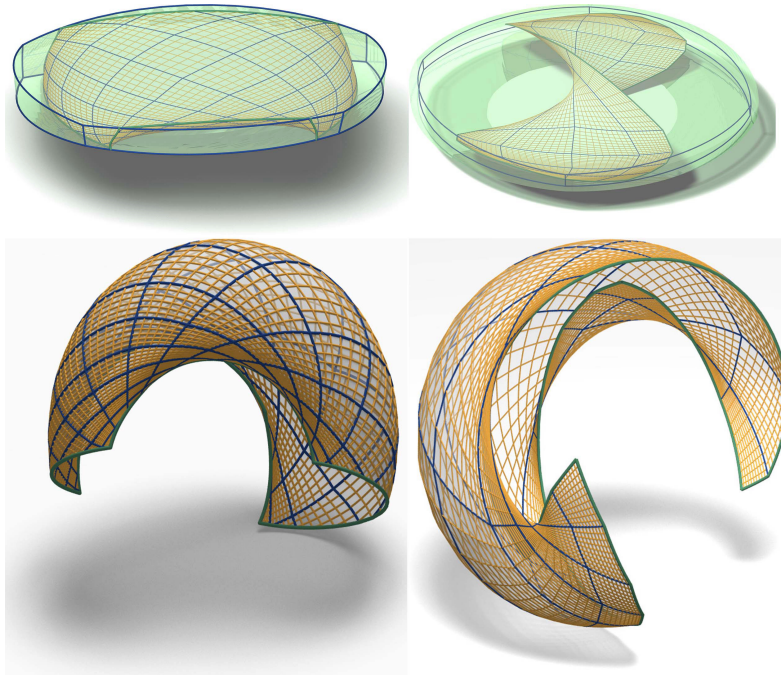


Figure 9: Darboux transformations map hyperbolic nets to smooth surfaces composed of Darboux cyclide patches. Top: To better understand the effect of the transformation, we embed the model to be transformed into a bounding box and show the transformed box. Bottom: One can clearly see that one is no longer restricted to surfaces with negative Gaussian curvature. The left images are obtained from the model in Fig. 5, middle row; the right images are D-transformed versions of the H-net in Fig. 5, bottom row.

general freeform surfaces. This may require an approach which avoids Darboux transformations and directly works with an appropriate control structure of the cyclide patches.

More generally, we are interested in smooth extensions of discrete structures – or slightly reformulated – in discrete structures which are actually smooth composites of simple elements. It could turn out that certain low degree spline curves and surfaces possess remarkable properties in discrete differential geometry, especially in those groups (affine, projective) where the classical theory requires higher order derivatives.

#### *Acknowledgments*

This research was supported in part by the DFG-Collaborative Research Center, TRR 109, *Discretization in Geometry and Dynamics*, through grant I 706-N26 of the Austrian Science Fund (FWF). We thank Udo Hertrich-Jeromin

and Johannes Wallner for stimulating discussions and the reviewers for their excellent comments and suggestions.

*Appendix: Proof of Theorem 6*

We use a local coordinate system with the flat point  $\mathbf{p}$  at the origin and with  $z = 0$  as tangent plane at  $\mathbf{p}$ . Locally, the surface can be written in Monge form,  $z = f(x, y)$ , and since  $z = 0$  is a 2nd order approximant, the Taylor expansion of  $f(x, y)$  starts with cubic terms (which do not vanish since the flat point is ordinary). Hence, it suffices to prove the result for the special surface,

$$z = f(x, y) = b_0x^3 + b_1x^2y + b_2xy^2 + b_3y^3. \quad (13)$$

There are 3 types of ordinary umbilics, which are sometimes called *star* (index  $-1/2$ ), *monstar* and *lemon* (both of index  $1/2$ ). The star type is characterized by (see [23]),

$$b_0b_2 - b_2^2 + b_1b_3 - b_1^2 < 0. \quad (14)$$

We claim that this inequality is always fulfilled since the flat point lies in a negatively curved area: Negative Gaussian curvature  $K$  is expressed by a negative determinant of the Hessian of  $f$ :  $f_{xx}f_{yy} - f_{xy}^2 < 0$ . For the surface (13), this condition reads

$$(3b_0b_2 - b_1^2)x^2 + (9b_0b_3 - b_1b_2)xy + (3b_1b_3 - b_2^2)y^2 < 0.$$

It has to hold for all  $(x, y) \neq (0, 0)$ , which implies

$$3b_0b_2 - b_1^2 < 0, \quad 3b_1b_3 - b_2^2 < 0,$$

and shows that (14) is satisfied.  $\diamond$

- [1] F. Käferböck, H. Pottmann, Smooth surfaces from bilinear patches: discrete affine minimal surfaces, *Computer-Aided Geom. Design* 30 (2013) 476–489.
- [2] M. Craizer, H. Anciaux, T. Lewiner, Discrete affine minimal surfaces with indefinite metric, *Differential Geometry and its Applications* 28 (2010) 158–169.
- [3] J. Wallner, H. Pottmann, Geometric computing for freeform architecture, *Journal of Math. in Industry* 1 (2011) #4,1–19.
- [4] A. Bobenko, Yu. Suris, *Discrete differential geometry: Integrable Structure*, American Math. Soc., 2008.
- [5] E. Huhnen-Venedey, T. Rörig, Discretization of asymptotic line parametrizations using hyperboloid surface patches, *Geometriae Dedicata* (to appear).

- [6] M. Eigensatz, M. Kilian, A. Schiftner, N. Mitra, H. Pottmann, M. Pauly, Paneling architectural freeform surfaces, *ACM Trans. Graphics* 29 (4) (2010) #45,1–10, *proc. SIGGRAPH*.
- [7] S. Flöry, Constrained matching of point clouds and surfaces, Ph.D. thesis, Vienna University of Technology (2010).
- [8] S. Flöry, H. Pottmann, Ruled surfaces for rationalization and design in architecture, *Proc. ACADIA* (2010) 103–109.
- [9] S. Flöry, Y. Nagai, F. Isvoranu, H. Pottmann, J. Wallner, Ruled free forms, in: L. Hesselgren, S. Sharma, J. Wallner, N. Baldassini, P. Bompas, J. Raynaud (Eds.), *Advances in Architectural Geometry*, Springer, 2012, pp. 57–66.
- [10] J. Wallner, On the semidiscrete differential geometry of A-surfaces and K-surfaces, *J. Geometry* 103 (2012) 161–176.
- [11] A. I. Bobenko, E. Huhnen-Venedey, Curvature line parametrized surfaces and orthogonal coordinate systems. Discretization with Dupin cyclides, *Geom. Dedicata* 159 (2012) 207–237.
- [12] P. Bo, H. Pottmann, M. Kilian, W. Wang, J. Wallner, Circular arc structures, *ACM Trans. Graphics* 30 (2011) #101,1–11, *Proc. SIGGRAPH*.
- [13] E. Huhnen-Venedey, W. K. Schief, On Weingarten transformations of hyperbolic nets, *Preprint* (2013).
- [14] H. Pottmann, L. Shi, M. Skopenkov, Darboux cyclides and webs from circles, *Computer-Aided Geom. Design* 29 (2012) 77–97.
- [15] F. Cazals, M. Pouget, Estimating differential quantities using polynomial fitting of osculating jets, in: *Symp. Geometry Processing, Eurographics*, 2003, pp. 177–187.
- [16] M. Zadavec, A. Schiftner, J. Wallner, Designing quad-dominant meshes with planar faces, *Computer Graphics Forum* 29 (5) (2010) 1671–1679.
- [17] B. Smyth, F. Xavier, A sharp geometric estimate for the index of an umbilic on a smooth surface, *Bull. London Math. Soc.* 24 (1992) 176–180.
- [18] F. Kälberer, M. Nieser, K. Polthier, Quadcover - surface parameterization using branched coverings, *Computer Graphics Forum* 26 (2007) 375–384.
- [19] D. Bommers, H. Zimmer, L. Kobbelt, Mixed-integer quadrangulation, *ACM Trans. Graph.* 28 (3) (2009) 77:1–77:10, *Proc. SIGGRAPH*.
- [20] Y. Liu, W. Xu, J. Wang, L. Zhu, B. Guo, F. Chen, G. Wang, General planar quadrilateral mesh design using conjugate direction field, *ACM Trans. Graph.* 30 (6) (2011) 140:1–140:10, *Proc. SIGGRAPH Asia*.

- [21] H. Pottmann, S. Leopoldseder, A concept for parametric surface fitting which avoids the parametrization problem, *Comput. Aided Geom. Design* 20 (2003) 343–362.
- [22] B. Deng, H. Pottmann, J. Wallner, Functional webs for freeform architecture, *Computer Graphics Forum* 30 (2011) 1369–1378, *Proc. Symp. Geometry Processing*.
- [23] F. Cazals, M. Pouget, Smooth surfaces, umbilics, lines of curvature, foliations, ridges and the medial axis: a concise overview, *INRIA Research Report* 5138 (2004).